Impact of *RUNX2* gene silencing on the gemcitabine sensitivity of *p53*-mutated pancreatic cancer MiaPaCa-2 spheres

MEIJIE SANG[1,2], MIZUYO NAKAMURA[1], TAKEHIRO OGATA[1], DAN SUN[3], OSAMU SHIMOZATO[1], TOSHIO NIKAIDO[2] and TOSHINORI OZAKI[1]

[1]Laboratory of DNA Damage Signaling, Chiba Cancer Center Research Institute, Chiba 260-8717; [2]Department of Regenerative Medicine, Graduate School of Medicine, University of Toyama, Toyama 930-0194, Japan; [3]Department of Urology, First Hospital of China Medical University, Shenyang, Liaoning110001, P.R. China

Received September 26, 2017; Accepted March 20, 2018

DOI: 10.3892/or.2018.6344

Abstract. Recently, it has been well-recognized that the response toward anticancer drugs differs between two- and three-dimensional (2D and 3D) *in vitro* cancer cell growth models. In the present study, we have demonstrated that, similar to the conventional 2D monolayer culture systems which often lack *in vivo* physiological insights, *RUNX2* gene silencing increases the gemcitabine (GEM) sensitivity of the 3D spheres generated from *p53*-mutated pancreatic cancer MiaPaCa-2 cells. According to our results, MiaPaCa-2 cells, but not *p53*-wild-type pancreatic cancer SW1990 cells efficiently formed sphere structures in serum-free sphere-forming medium. Although GEM treatment caused a marked induction of TAp73/TAp63 in MiaPaCa-2 spheres accompanied by the transcriptional activation of p53 family-target genes such as $p21^{WAF1}$ and *NOXA*, only 20% of cells underwent cell death. Under these experimental conditions, mutant p53 expression level was increased in response to GEM and RUNX2 remained unchanged at the protein level regardless of GEM exposure, which may suppress the pro-apoptotic activity of TAp73/TAp63. Notably, *RUNX2* gene silencing markedly augmented GEM-mediated cell death of MiaPaCa-2 spheres compared to that of non-depleted ones. Expression analyses revealed that forced depletion of *RUNX2* further stimulated GEM-induced upregulation of TAp63 as well as its downstream target genes such as $p21^{WAF1}$ and *NOXA*. In summary, our observations strongly indicated that, similarly to 2D monolayer culture, *RUNX2* gene silencing increased GEM sensitivity of MiaPaCa-2 spheres and highlighted the therapeutic potential of RUNX2 in pancreatic cancer with *p53* mutation.

Correspondence to: Dr Toshinori Ozaki, Laboratory of DNA Damage Signaling, Chiba Cancer Center Research Institute, 666-2 Nitona, Chuoh-ku, Chiba 260-8717, Japan
E-mail: tozaki@chiba-cc.jp

Abbreviations: DTT, dithiothreitol; EGF, epidermal growth factor; EMT, epithelial-mesenchymal transition; bFGF, fibroblast growth factor-basic; GEM, gemcitabine; MRP5, multidrug resistant protein 5; PARP, poly (ADP-ribose) polymerase; PI, propidium iodide; RPM2, ribonucleotide reductase M2; RUNX2, runt-related transcription factor 2; siRNA, small interfering RNA; TBS, Tris-buffered saline

Key words: gemcitabine, pancreatic cancer, p53 family, RUNX2, sphere

Introduction

Pancreatic cancer is the fourth leading cause of cancer-related deaths in Japan and its overall 5-year survival rate remains very low (less than 10%) (1). Although surgical resection provides complete cure for patients with pancreatic cancer, over 80% of cases are judged to be inoperable at the time of initial diagnosis, due to advanced disease or distant metastasis, and thus subjected to chemotherapy and/or radiotherapy (2). The DNA damaging anticancer drug, gemcitabine (GEM) is a first-line chemotherapy agent for patients. However, most of them do not respond well to GEM treatment, followed by subsequent disease progression (3,4). To overcome this serious issue, a variety of combinations of GEM with other anticancer drugs such as Nab-paclitaxel (Nab-P) and 5-fluorouracil (5-FU) have been assessed. Unfortunately, these combinations have resulted in limited clinical benefits for patients compared to patients treated with GEM alone (5). Since the vast majority of cases carry loss of function mutations in tumor suppressor gene *p53*, as well as *CDKN2A* and gain of function (GOF) mutations in proto-oncogene K-*Ras* (6), it is probable that these mutations may contribute to the acquisition of resistance of pancreatic cancer tissues to GEM. Considering this, the understanding of the precise molecular basis behind the GEM-resistant property of pancreatic cancer is urgently required.

RUNX2 (runt-related transcription factor 2) has been widely accepted to be one of the master regulators of osteoblast differentiation and bone formation. Previous studies have revealed that *RUNX2*-deficient mice lack a mineralized skeleton and its forced expression potentiates the osteoblast transcription program (7,8). As expected, RUNX2 transactivates its multiple downstream target gene promoters implicated in osteogenesis such as osteocalcin (OCN), type I collagen, osteopontin (OPN) and collagenase 3 (9). In addition to osteogenesis, a growing

body of evidence indicates that RUNX2 has a pro-oncogenic function. For example, RUNX2 has been demonstrated to be aberrantly overexpressed in numerous cancer tissues compared to their corresponding normal ones (10). Consistent with these observations, forced expression and depletion of RUNX2 promoted and suppressed malignant phenotypes of cancer cells of various origins, respectively (10,11).

Recently, we have demonstrated that *RUNX2* gene silencing significantly increased chemosensitivity of human osteosarcoma and pancreatic cancer cells through the augmentation of the tumor suppressor p53 family-dependent cell death pathway (12-15). Tumor suppressor p53 family is composed of three members including p53, TAp73 and TAp63 (16,17). According to our observations, *RUNX2* knockdown markedly increased GEM sensitivity of *p53*-mutated pancreatic cancer cells (14,15). Since it has been well known that mutant p53 with an extended half-life participates in the acquisition/maintenance of chemoresistant properties of aggressive cancers (16,18), it is indicative that depletion of *RUNX2* may override at least in part, the negative effect of mutant p53 on their chemosensitivity. To further validate our prior results, we sought to address these issues under the anchorage-independent growth of pancreatic cancer cells (spheres) instead of the conventional two-dimensional (2D) monolayer culture conditions (19). It has been considered that multicellular spheres mimic the *in vivo* physiological microenvironments of cancer tissues (20).

In the present study, we took advantage of the clinically-relevant *in vitro* sphere culture system and demonstrated that *RUNX2* gene silencing increased the GEM sensitivity of *p53*-mutated pancreatic cancer MiaPaCa-2 spheres through the stimulation of TAp63-dependent cell death pathway.

Materials and methods

Cells and cell culture. Human pancreatic cancer-derived SW1990 and MiaPaCa-2 cells obtained from The American Type Culture Collection (Manassas, VA, USA) were maintained in Dulbecco's modified Eagle's medium (DMEM; Wako Pure Chemical Industries, Ltd., Osaka, Japan) supplemented with heat-inactivated 10% fetal bovine serum (FBS; Invitrogen; Thermo Fisher Scientific, Inc., Carlsbad, CA, USA) and 50 units/ml of penicillin/streptomycin. The cells were cultured in incubators with a humidified atmosphere of 5% CO_2 and 95% air, at 37˚C.

Sphere formation. Cells were suspended in serum-free sphere medium DMEM/F12 (Wako Pure Chemical Industries, Ltd., Osaka, Japan) supplemented with B27 (Bay Bioscience, Co., Ltd., Tokyo, Japan), 25 ng/ml of basic FGF (bFGF; Miltenyi Biotec, Tokyo, Japan) and 20 ng/ml of EGF (Miltenyi Biotec) and seeded in 6-well plates at a density of $5x10^5$ cells/well. At the indicated time-points after seeding (day 0, day 1, day 2 and day 3), representative images were captured.

siRNA-mediated knockdown. For siRNA-mediated silencing of *RUNX2*, MiaPaCa-2 spheres were transfected with control siRNA (Santa Cruz Biotechnology, Santa Cruz, CA, USA) or with siRNA targeting *RUNX2* (Dharmacon; Ge Healthcare, Lafayette, CO, USA) using Lipofectamine 2000 transfection reagent according to the manufacturer's instructions (Invitrogen; Thermo Fisher Scientific, Inc.). The final concentration of each siRNA was 10 nM. *RUNX2* gene silencing was evaluated by immunoblotting and RT-PCR.

Immunoblotting. Cells were lysed in 1X Laemmli buffer supplemented with 0.1 M DTT and the commercial protease inhibitor mixture (product no. P8340; Sigma-Aldrich; Merck KGaA, Darmstadt, Germany). Equal amounts of cell lysates (30 μg of protein) were analyzed by 10% SDS-polyacrylamide gel electrophoresis, transferred onto membrane filter (Immobilon; Merck Millipore, Amsterdam, The Netherlands), and incubated with Tris-buffered saline containing 0.1% Tween-20 (TBS-T) plus 5% of non-fat dry milk at 4˚C overnight. The membranes were probed with mouse monoclonal anti-p53 (DO-1; 1:4,000; cat. no. sc126; Santa Cruz Biotechnology) which recognizes both wild-type and mutant p53, rabbit polyclonal anti-TAp73 (1:1,000; cat. no. GTX-109045; GeneTex, Inc., Irvine, CA, USA), rabbit polyclonal anti-TAp63 (1:1,000; cat. no. GTX-102425; GeneTex), rabbit monoclonal anti-RUNX2 (1:1,000; cat. no. 8486; Cell Signaling Technology, Beverley, CA, USA), rabbit polyclonal anti-E2F-1 (1:1,000; cat. no. 3742; Cell Signaling Technology), rabbit polyclonal anti-PARP (1:1,000; cat. no. 9542; Cell Signaling Technology), mouse monoclonal anti-Itch (1:2,000; cat. no. 611199; BD Transduction Laboratories, Lexington, KY, USA), mouse monoclonal anti-Lamin B (1:2,000; cat. no. NA12; 101-B7; Calbiochem; Merck KGaA, St. Louis, MO, USA), mouse monoclonal anti-γH2AX (2F3; 1:2,000; cat. no. 613401; BioLegend, San Diego, CA, USA) or with mouse monoclonal anti-actin antibody (C-2; 1:2,000; cat. no. sc-8432; Santa Cruz Biotechnology) at room temperature for 1 h. Actin was used as a loading control. After washing in TBS-T, the membranes were incubated with horseradish peroxidase-conjugated goat anti-mouse (cat. no. 31430) or anti-rabbit IgG (cat. no. 31466) (1:4,000; Invitrogen; Thermo Fisher Scientific, Inc.) at room temperature for 1 h. Immunoreactive signals were detected with an enhanced chemiluminescence detection system (ECL; Ge Healthcare Life Science, Piscataway, NJ, USA).

RNA preparation and RT-PCR. Total RNA was extracted from the indicated cells using RNeasy Mini kit following the manufacturer's instructions (Qiagen, Valencia, CA, USA). One microgram of total RNA was reverse-transcribed using SuperSprict VILO cDNA Synthesis system (Invitrogen; Thermo Fisher Scientific, Inc.) according to the manufacturer's protocol. The resultant cDNA was subsequently used as a template for PCR-based amplification with gene-specific primer sets. Gene expression was normalized relative to that of the housekeeping gene *GAPDH*. The oligonucleotide primers used for PCR were as follows: *p53* forward, 5'-CTGCCCTCA ACAAGATGTTTTG-3' and reverse, 5'-CTATCTGAGCAG CGCTCATGG-3'; *TAp63* forward, 5'-GACCTGAGTGAC CCCATGTG-3' and reverse, 5'-CGGGTGATGGAGAGA GAGCA-3'; *TAp73* forward, 5'-TCTGGAACCAGACAGCAC CT-3' and reverse, 5'-GTGCTGGACTGCTGGAAAGT-3'; *RUNX2* forward, 5'-TCTGGCCTTCCACTCTCAGT-3' and reverse, 5'-GACTGGCGGGGTGTAAGTAA-3'; $p21^{WAF1}$ forward, 5'-ATGAAATTCACCCCCTTTCC-3' and reverse,

5'-CCCTAGGCTGTGCTCACTTC-3'; *NOXA* forward, 5'-CTGGAAGTCGAGTGTGCTACT-3' and reverse 5'-TCAGGTTCCTGAGCAGAAGAG-3'; *BAX* forward, 5'-AGAGGATGATTGCCGCCGT-3' and reverse, 5'-CAACCACCCTGGTCTTGGAT-3'; *PUMA* forward, 5'-GCCCAGACTGTGAATCCTGT-3' and reverse, 5'-TCCTCCCTCTTCCGAGATTT-3'; *Itch* forward, 5'-ACCTGGATGGGAGAAGAGAA-3' and reverse, 5'-TGTGCGGGGATCTATATAGG-3'; *GAPDH* forward, 5'-ACCTGACCTGCCGTCTAGAA-3' and reverse, 5'-TCCACCACCCTGTTGCTGTA-3'. PCR products were analyzed by 1.5% agarose gel electrophoresis and visualized using ethidium bromide staining (Wako Pure Chemical Industries, Ltd.).

WST cell survival assay. Cell viability was determined by standard WST cell survival assay. In brief, $5x10^3$ cells were seeded in triplicate in 96-well plates and allowed to attach overnight. Cells were then treated with or without the indicated concentrations of GEM. Forty-eight hours after GEM exposure, their proliferation was assesed by Cell Counting Kit-8 (CCK-8) reagent (Dojindo Molecular Technologies, Kumamoto, Japan) following the manufacturer's instructions.

Trypan blue dye exclusion assay. Cells were exposed to the indicated concentrations of GEM. Forty-eight hours after treatment, floating and adherent cells were collected and incubated with 0.4% trypan blue solution (Bio-Rad Laboratories, Hercules, CA, USA) at room temperature for 3 min. The reaction mixtures were then subjected to a TC20 automated cell counter (Bio-Rad Laboratories). Trypan blue-positive and -negative cells were considered to be dead and viable cells, respectively.

Flow cytometric analysis. Forty-eight hours after GEM exposure, floating and attached cells were harvested, washed in 1X phosphate-buffered saline (PBS) and fixed in ice-cold 70% ethanol. After fixation, cells were treated with 1 mg/ml of propidium iodide (PI) and 1 μg/ml of RNase A at 37˚C for 30 min in the dark. The cells were then analyzed by flow cytometry (FACSCalibur; BD Biosciences, Franklin Lakes, NJ, USA).

Statistical analysis. The results were presented as the mean ± SD of three independent experiments. One-way ANOVA tests were performed to determine the statistical significance of difference among the control and treated groups using Ekuseru-Toukei 2010 software (Social Survey Research Information Co., Ltd., Tokyo, Japan). $P<0.05$ was considered to indicate a statistically significant difference.

Results

p53-mutated pancreatic cancer MiaPaCa-2 cells but not p53-wild-type pancreatic cancer SW1990 cells, form sphere structure. Considering that ~75% of pancreatic cancer tissues carry *p53* mutations and exhibit a serious anticancer drug resistance (6), we sought to compare GEM sensitivity between *p53*-wild-type and *p53*-mutated pancreatic cancer cells under the conventional monolayer culture conditions. As clearly displayed in Figs. 1 and 2, *p53*-mutated MiaPaCa-2 cells poorly responded to GEM compared to *p53*-wild-type pancreatic cancer SW1990 cells ($P<0.01$), indicating that *p53* mutation may be involved in the lower GEM sensitivity of pancreatic cancer cells.

Recently, it has been increasingly recognized that the response rate of cancer cells to anticancer drugs differs between two- and three-dimensional (2D and 3D) cancer cell growth models. Among 3D cultures ranging in complexity from layered cellular systems to complex multi-cell type spheres, 3D sphere cultures mimic the architectures and cellular contacts of cells in cancer tissues (20). These findings prompted us to evaluate the GEM sensitivity of spheres generated from MiaPaCa-2 and SW1990 cells, and compare it to that of 2D monolayer cultures. Firstly, we questioned whether MiaPaCa-2 and SW1990 cells could form 3D spheres. The indicated numbers of MiaPaCa-2 cells were cultured in the standard medium-containing serum, and then transferred into serum-free sphere-forming medium. At the indicated time-points following incubation in the sphere-forming medium, representative images were captured. As displayed in Fig. 3A-C, MiaPaCa-2 cells ($5x10^5$ and $1x10^6$ cells/plate) gave rise to obvious multi-cellular structures under our experimental conditions. In contrast to MiaPaCa-2, SW1990 cells did not form sphere structures until 3 days of incubation (Fig. 3D), indicating that *p53* status may be involved in sphere formation of pancreatic cancer cells.

Under the same experimental conditions, cell lysates and total RNA were prepared from MiaPaCa-2 spheres and analyzed by immunoblotting and RT-PCR, respectively. As displayed in Fig. 4, the expression levels of mutant p53, TAp73 and TAp63 proteins were elevated during the sphere formation. RT-PCR analysis revealed that p53 family target gene transcription was markedly reduced in MiaPaCa-2 spheres compared to that of the adherent MiaPaCa-2 cells (day 0), indicating that mutant p53 prohibited the transcriptional activity of TAp73/TAp63.

MiaPaCa-2 spheres respond poorly to GEM. Since it has been demonstrated that spheres often display the lower sensitivity to anticancer drugs (21,22), we thus examined the cytotoxic effect of GEM on MiaPaCa-2 spheres. To this end, MiaPaCa-2 cells were cultured in sphere-forming medium and then exposed to different concentrations of GEM up to 10 μM. At the indicated time-points after treatment, the cells were analyzed by trypan blue dye exclusion assay. Although MiaPaCa-2 spheres underwent cell death following GEM exposure, there were no marked differences in dose response among MiaPaCa-2 spheres at a dose range of 2.5-10 μM of GEM (Fig. 5). Therefore, for further experiments, we treated MiaPaCa-2 spheres with 2.5 μM of GEM for 48 h. Under these experimental conditions, representative images were captured and the spheres were subsequently subjected to FACS analysis. As displayed in Fig. 6A, GEM treatment caused at most 2-fold increase in the number of cells with sub-G_1 DNA content relative to the untreated ones, which was almost in accordance with the results obtained from the trypan blue dye exclusion assay.

To gain an insight into understanding the molecular basis behind the poor response of MiaPaCa-2 spheres to GEM, the expression patterns of p53 family members and their target genes were examined. As displayed in Fig. 6B, the amount of

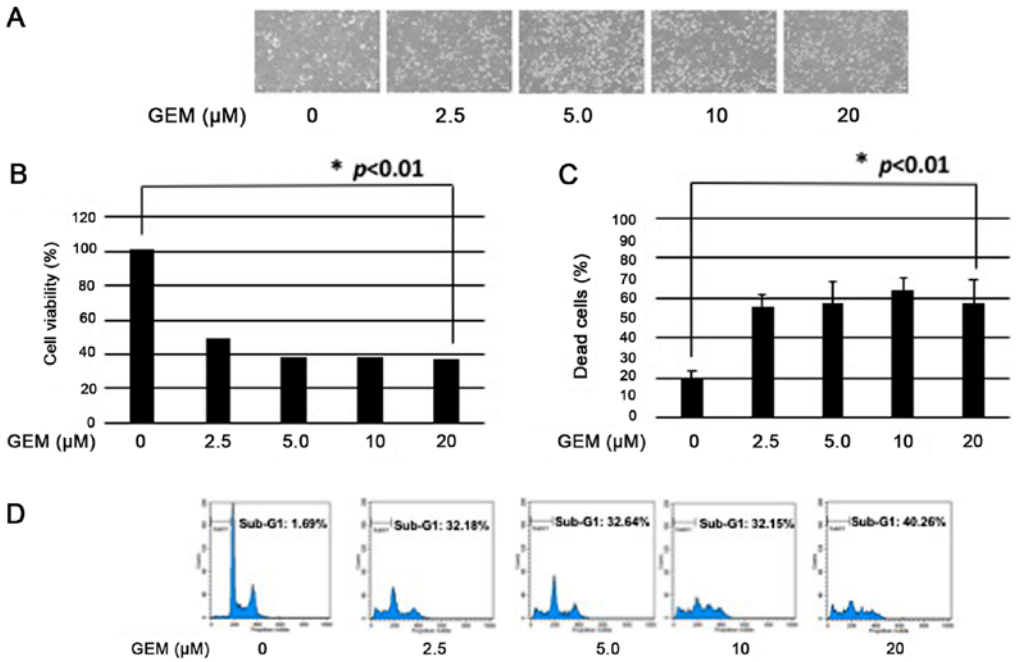

Figure 1. Higher sensitivity of *p53*-wild-type pancreatic cancer SW1990 cells to GEM. (A) SW1990 cells were treated with the indicated concentrations of GEM. Forty-eight hours after treatment, representative images were captured. (B) WST cell survival assay. SW1990 cells were treated as described in (A). Forty-eight hours after GEM treatment, cell viability was assessed by standard WST assay (*P<0.01). (C) Trypan blue dye exclusion assay. SW1990 cells were treated as described in (A). Forty-eight hours after GEM exposure, cells were processed for trypan blue dye exclusion assay. The number of trypan blue-positive (dead) cells was assessed (*P<0.01). (D) FACS analysis. SW1990 cells were treated as described in (A). Forty-eight hours post treatment, floating and attached cells were collected and subjected to flow cytometric analysis.

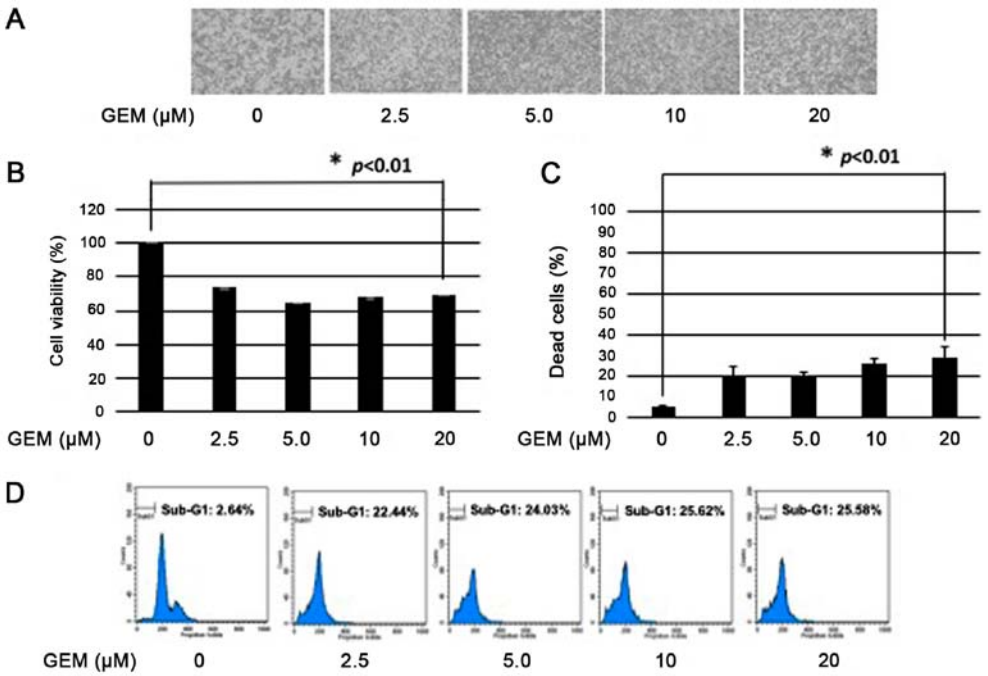

Figure 2. Lower sensitivity of *p53*-mutated pancreatic cancer MiaPaCa-2 cells to GEM. (A) MiaPaCa-2 cells were exposed to increasing concentrations of GEM. Forty-eight hours after treatment, representative images were captured. (B) WST cell survival assay. MiaPaCa-2 cells were treated as described in (A). Forty-eight hours after GEM treatment, cell viability was assessed by standard WST assay (*P<0.01). (C) Trypan blue dye exclusion assay (*P<0.01). MiaPaCa-2 cells were treated as described in (A). Forty-eight hours after GEM exposure, cells were mixed with 0.4% trypan blue solution and the number of trypan blue-positive (dead) cells was determined. (D) FACS analysis. MiaPaCa-2 cells were treated as in (A). Forty-eight hours after GEM treatment, floating and attached cells were collected and subjected to flow cytometric analysis.

γH2AX, which is one of the reliable molecular markers for DNA damage, was increased following GEM exposure in a dose-dependent manner, indicating that MiaPaCa-2 spheres received DNA damage. In addition, the proteolytic cleavage

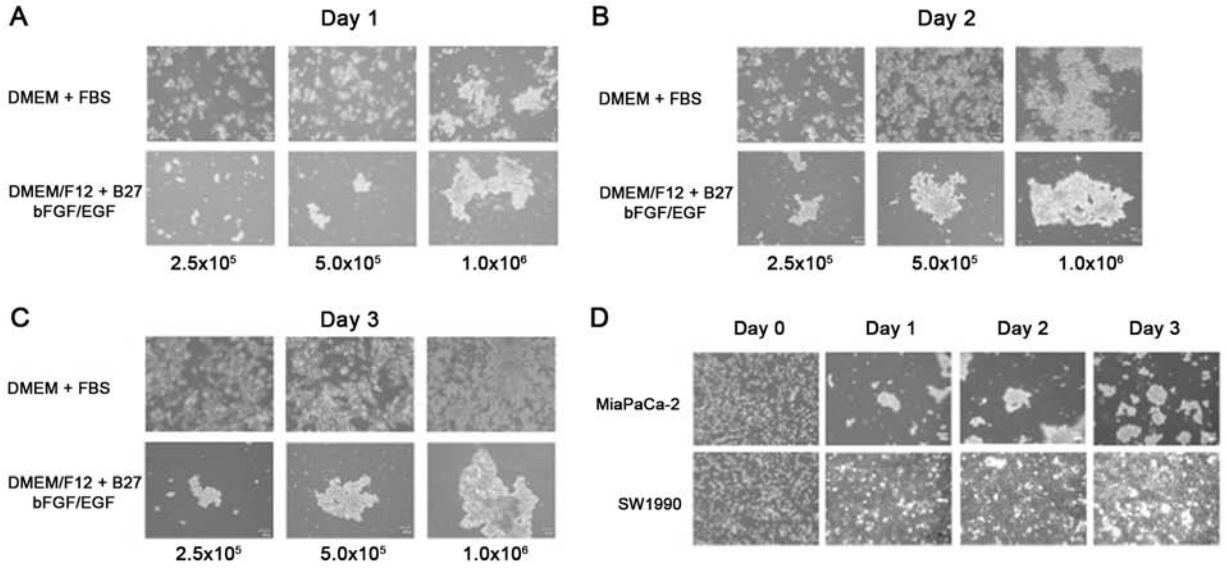

Figure 3. MiaPaCa-2 cells, but not SW1990 cells, form sphere structures *in vitro*. (A-C) The indicated numbers of MiaPaCa-2 cells were cultured in conventional medium containing serum (DMEM/FBS) (upper panels) or in serum-free sphere-forming medium (DMEM/F12/B27/bFGF/EGF) (lower panels). At the indicated time-points after the incubation, representative images were captured. (D) MiaPaCa-2 and SW1990 cells ($5x10^5$ cells/6-well plate) were cultured in sphere-forming medium. At the indicated time-points after the incubation, representative images were captured.

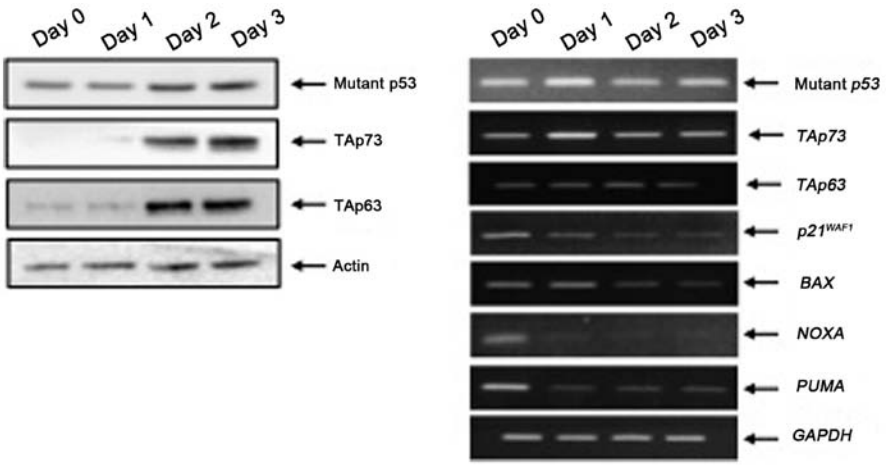

Figure 4. Elevated expression of mutant p53, TAp73 and TAp63 proteins during MiaPaCa-2 sphere formation. MiaPaCa-2 cells ($5x10^5$ cells/6-well plate) were cultured in sphere-forming medium (as described in Fig. 3D). At the indicated time-points after incubation, cell lysates and total RNA were prepared and analyzed by immunoblotting (left panels) and RT-PCR (right panels), respectively. Actin and *GAPDH* were used as a loading and an interenal control, respectively.

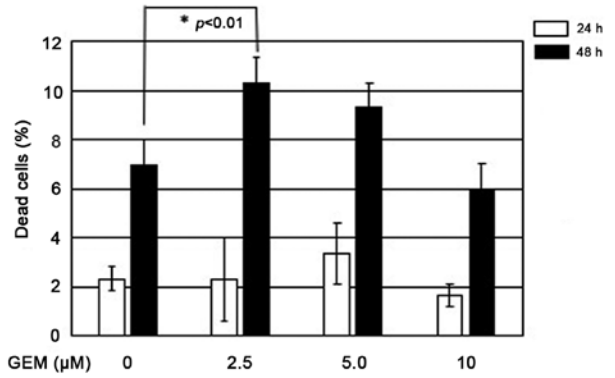

Figure 5. Poor response of MiaPaCa-2 spheres to GEM. MiaPaCa-2 cells were cultured in sphere-forming medium and then exposed to increasing concentrations of GEM. At the indicated time-points after treatment, spheres were collected and subjected to trypan blue dye exclusion assay (*P<0.01).

of PARP which may be catalyzed by the activated caspase-3, was detectable at 48 h after GEM treatment. For p53 family members, mutant p53, TAp73 and TAp63 proteins were upregulated in response to GEM. Since E2F-1, which acts as a transcriptional activator of TAp73 (23), was significantly induced following GEM exposure, it is likely that E2F-1 is responsible for the GEM-mediated induction of TAp73. Concurrently, RUNX2 remained basically unchanged regardless of the GEM treatment. RT-PCR analysis demonstrated that GEM treatment stimulated the transcription of *p53* family members (mutant *p53* and *TAp73*) as well as *E2F-1* (Fig. 6C). By contrast, *TAp63* was unaffected by GEM. For p53 family-target genes, GEM-mediated transcriptional activation of $p21^{WAF1}$ and *NOXA* was observed, whereas we did not detect a significant change in the expression levels of *BAX* and *PUMA* in response to GEM. As displayed in Fig. 6B, the amount of

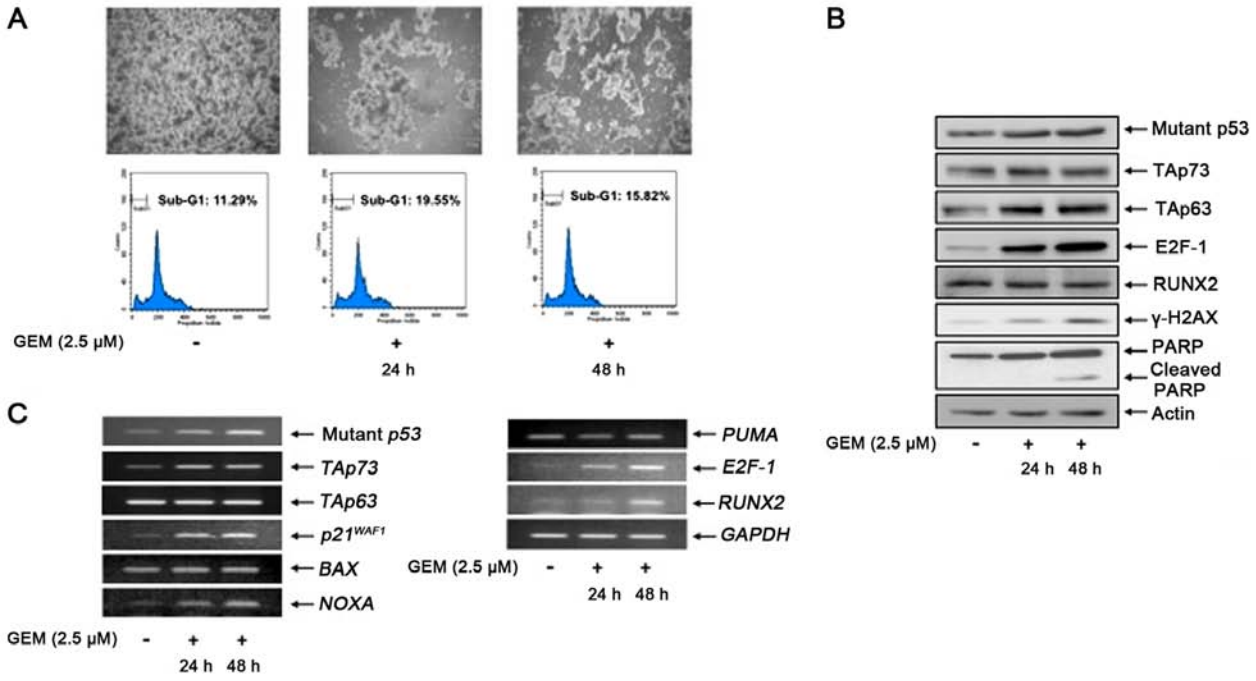

Figure 6. GEM-mediated upregulation of mutant p53, TAp73 and TAp63 proteins in MiaPaCa-2 spheres. (A) MiaPaCa-2 spheres were treated with 2.5 μM of GEM or left untreated. At the indicated time-points after GEM exposure, representative images were captured (upper panels), and then spheres were subjected to FACS analysis (lower panels). (B and C) MiaPaCa-2 spheres were treated as described in (A). Forty-eight hours after treatment, cell lysates and total RNA were prepared and analyzed by immunoblotting (B) and RT-PCR (C), respectively. Actin and *GAPDH* were used as a loading and an internal control, respectively.

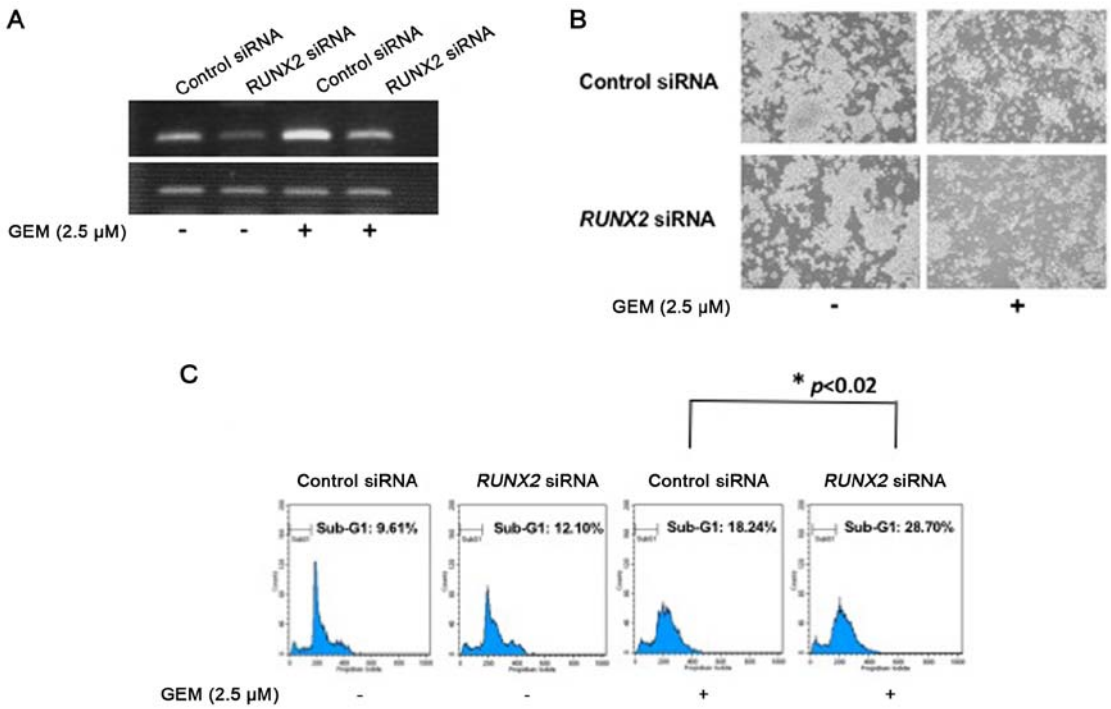

Figure 7. Depletion of *RUNX2* increases GEM sensitivity of MiaPaCa-2 spheres. (A) RT-PCR. MiaPaCa-2 spheres were transfected with non-targeting control siRNA or with siRNA against *RUNX2*. Twenty-four hours after transfection, the spheres were treated with or without 2.5 μM of GEM. Forty-eight hours after treatment, total RNA was isolated and analyzed for *RUNX2* by RT-PCR. *GAPDH* was used as an internal control. (B and C) *RUNX2* depletion-mediated enhancement of GEM sensitivity of MiaPaCa-2 spheres. MiaPaCa-2 spheres were transfected as described in (A). Twenty-four hours after transfection, the spheres were treated with or without 2.5 μM of GEM. Forty-eight hours after GEM exposure, (B) representative images were captured, and then (C) the spheres were harvested and subjected to FACS analysis (*P<0.02).

RUNX2 protein remained constant in the presence or absence of GEM, whereas GEM treatment led to a marked increase in *RUNX2* transcription level. At present, we do not know the molecular mechanism(s) underlying this discrepancy.

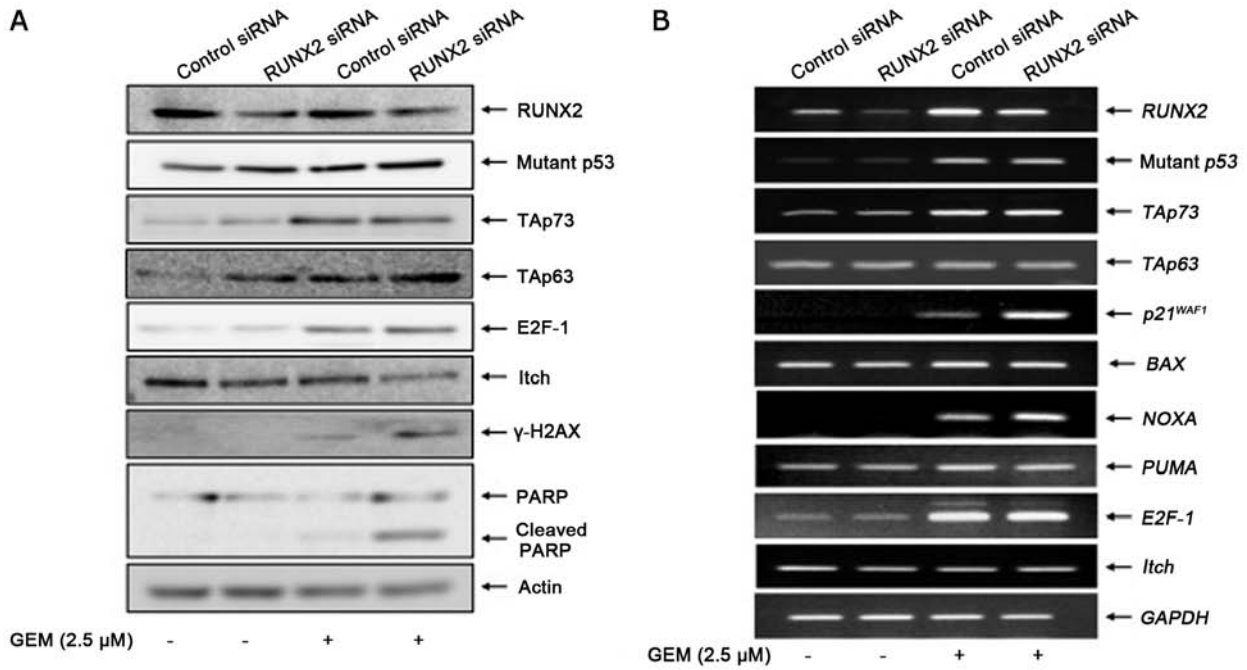

Figure 8. Silencing of *RUNX2* further potentiates GEM-mediated TAp63 protein accumulation in MiaPaCa-2 spheres. (A and B) MiaPaCa-2 spheres were transfected as in described in Fig. 7A. Twenty-four hours post transfcetion, the spheres were exposed to 2.5 μM of GEM or left untreated. Forty-eight hours after treatment, cell lysates and total RNA were prepared and analyzed by (A) immunoblotting and (B) RT-PCR, respectively. Actin and *GAPDH* were used as a loading and an internal control, respectively.

Based on these expression analyses, it is probable that, despite GEM-mediated stimulation of TAp73/TAp63 expression, poor response of MiaPaCa-2 spheres to GEM may be due to GEM-induced further accumulation of mutant p53 and/or the constitutive expression of RUNX2.

Knockdown of RUNX2 increases the GEM sensitivity of MiaPaCa-2 spheres. Recently, we have revealed that *RUNX2* knockdown sensitizes MiaPaCa-2 cells to GEM under the conventional 2D monolayer culture conditions (14). To examine the possible impact of RUNX2 on the GEM sensitivity of MiaPaCa-2 spheres, siRNA-mediated depletion of *RUNX2* was performed. As displayed in Fig. 7A, *RUNX2* gene silencing was successful under our experimental conditions as verified by RT-PCR analysis. Twenty-four hours after the siRNA transfection, MiaPaCa-2 spheres were exposed to 2.5 μM of GEM or left untreated. Forty-eight hours after treatment, representaive images were captured and spheres were processed for the subsequent FACS analysis. As clearly displayed in Fig. 7B, GEM-induced decrease in the number of spheres and disruption of their multi-cellular structures were augmented by *RUNX2* depletion. Furthermore, FACS analysis demonstrated that *RUNX2* knockdown increased the number of cells with sub-G_1 DNA content of MiaPaCa-2 spheres in response to GEM compared to non-silencing ones exposed to GEM (Fig. 7C). These results indicated that, similar to 2D monolayer cultures (14), *RUNX2* gene silencing increased the sensitivity of MiaPaCa-2 spheres to GEM.

RUNX2 depletion causes further augmentation of the GEM-mediated accumulation of TAp63 protein in MiaPaCa-2 spheres. To investigate the molecular mechanism(s) by which *RUNX2* gene silencing increased the GEM sensitivity of MiaPaCa-2 spheres, we examined the expression patterns of the p53 family members and their target genes in *RUNX2*-depleted spheres in response to GEM. In support of the results obtained by FACS analysis, GEM-mediated proteolytic cleavage of PARP was markedly stimulated in *RUNX2*-silencing MiaPaCa-2 spheres (Fig. 8A). Notably, *RUNX2* depletion augmented GEM-induced accumulation of γH2AX, while, *RUNX2* gene silencing had a negligible effect on GEM-mediated induction of mutant p53, TAp73 and E2F-1 proteins. Unlike TAp73 protein, GEM-dependent promotion of the TAp63 protein expression was further stimulated by *RUNX2* knockdown. In accordance with these results, Itch which acts as an E3 ubiquitin protein ligase for TAp63 (24), was downregulated in *RUNX2*-silencing spheres exposed to GEM. RT-PCR analyses demonstrated that GEM-mediated transcriptional activation of mutant *p53*, *TAp73* and *E2F-1* was unaffected by *RUNX2* depletion (Fig. 8B). Among the p53 family-target genes that we examined, *RUNX2* knockdown further stimulated GEM-induced upregulation of *p21*^{WAF1} and *NOXA*. *TAp63* and *Itch* remained unchanged regardless of GEM treatment or *RUNX2* depletion, raising a possibility that TAp63 was regulated by RUNX2 at the protein level under sphere culture. As displayed in Fig. 9A, TAp63 protein was stabilized in MiaPaCa-2 spheres in the presence of proteasome inhibitor MG-132. Notably, forced expression of RUNX2 in MiaPaCa-2 spheres reduced TAp63 at the protein level but not at the mRNA level (Fig. 9B). Collectively, these results demonstrated that knockdown of *RUNX2* stabilized TAp63, potentiated TAp63-dependent cell death pathway in MiaPaCa-2 spheres, thereby increasing their GEM sensitivity.

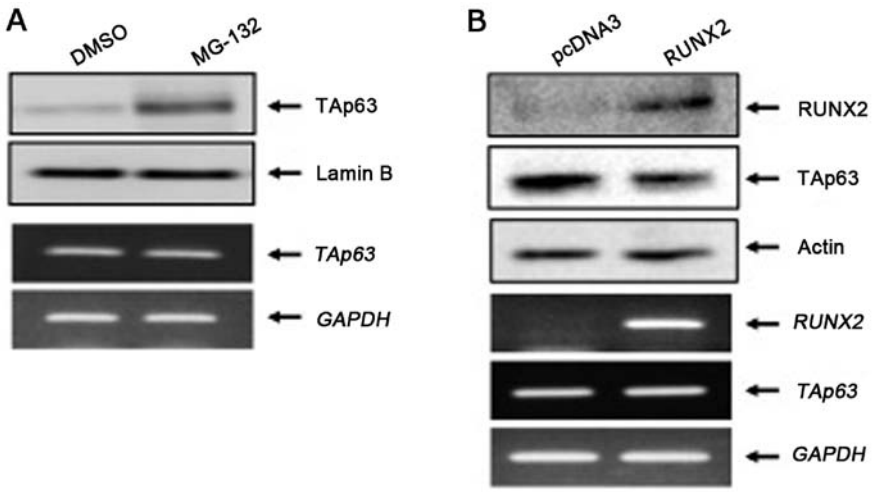

Figure 9. RUNX2 promotes the degradation of TAp63 protein. (A) MiaPaCa-2 spheres were treated with DMSO or with MG-132 (10 μM). Six hours after treatment, cell lysates and total RNA were prepared and analyzed by immunoblotting (upper panels) and RT-PCR (lower panels), respectively. Lamin B and *GAPDH* were used as a loading and an interenal control, respectively. (B) MiaPaCa-2 spheres were tranfected with the empty plasmid (pcDNA3) or with the expression plasmid for RUNX2. Forty-eight hours after transfection, cell lysates and total RNA were prepared and analyzed by immunoblotting (upper panels) and RT-PCR (lower panels), respectively. Actin and *GAPDH* were used as a loading and an internal control, respectively.

Discussion

In the present study, we have demonstrated that, similar to the conventional 2D cell culture model, *RUNX2* gene silencing increased the GEM sensitivity of *p53*-mutated pancreatic cancer MiaPaCa-2 cells under the non-adherent 3D sphere system. Therefore, we propose that *RUNX2* may serve as a potential therapeutic target of pancreatic cancer.

According to our results, MiaPaCa-2 cells poorly responded to GEM compared to SW1990 cells under the adherent 2D culture conditions. Notably, MiaPaCa-2 cells efficiently formed spheres, whereas SW1990 cells did not, indicating that *p53* status is involved in the formation of pancreatic cancer cell spheres. In support of this notion, *p53*-mutated pancreatic cancer Panc-1 cells also generated the sphere structures under our experimental conditions (data not shown). Recently, Ren *et al* (25) described that wild-type p53 suppressed epithelial-mesenchymal transition (EMT) of prostate cancer cells through the downregulation and upregulation of the expression of mesenchymal and epithelial markers, respectively. Additionally, they have also revealed that prostate cancer cell sphere formation was markedly suppressed by wild-type p53. Alternatively, Cho *et al* (26) successfully generated spheres from the adherent pancreatic cancer CFPAC-1 and CAPAN-1 cells bearing *p53* mutation in serum-free medium. Based on their observations, CFPAC-1 spheres highly expressed pro-oncogenic PAUF (pancreatic adenocarcinoma upregulated factor) relative to the adherent CFPAC-1 cells and *PAUF* gene silencing resulted in a decrease in the number of spheres and an enhancement of chemotherapeutic response to GEM in association with downregulation of MRP5 (multidrug resistant protein 5) and RPM2 (ribonucleotide reductase M2). Similar results were also obtained in *p53*-mutated pancreatic cancer BxPC-3 cells (27). Notably, Di Fiore *et al* (28) described that ectopic expression of mutant p53 (R248W) in osteosarcoma cells promoted cancer stem cell (CSC)-like features such as sphere formation, indicating that certain gain of function (GOF) mutants of p53 contributed to efficient sphere generation in the absence of serum. Therefore, it is likely that certain GOF mutants of p53-induced sphere-forming ability in malignant cancer cells may be one of their strategies to survive under the severe environments such as low nutrient. From our expression analyses, mutant p53 expression was elevated in MiaPaCa-2 spheres relative to the adherent MiaPaCa-2 cells accompanied by a significant reduction in p53-target gene transcription such as $p21^{WAF1}$, *BAX*, *PUMA* and *NOXA*. Considering that mutant p53 acts as a dominant-negative inhibitor against the other pro-apoptotic p53 family members such as TAp73 and TAp63, it is possible that the collaboration of mutant p53 with PAUF and/or mutant p53-dependent inhibition of TAp73/TAp63 activity may participate in the regulatory mechanism of sphere formation as well as GEM resistance. Further experiments are required to adequately address this issue.

As suggested by Kuo *et al* (22), 3D sphere cultures may reflect the *in vivo*-like microenvironments more effectively than the conventional 2D adherent ones. This sphere culture system takes into account the critical interaction of cells with their neighbors and their environments. According to our results, at most 20% of MiaPaCa-2 spheres underwent cell death in response to GEM. The adherent MiaPaCa-2 cells displayed a lower sensitivity to GEM than the monolayer SW1990 cells. Under the sphere culture conditions, GEM exposure resulted in an upregulation of mutant p53, TAp73, TAp63 proteins and p53 family-target genes such as $p21^{WAF1}$ and *NOXA*, while, RUNX2 protein level remained unchanged regardless of the GEM treatment. As previously described (13,14), RUNX2 was capable of attenuating the pro-apoptotic activity of TAp73/TAp63, therefore it is likely that, in addition to mutant p53, RUNX2 prohibited TAp73/TAp63 activity under non-adherent 3D cultures. In a good agreement with this notion, *RUNX2* gene silencing improved GEM sensitivity of MiaPaCa-2 spheres in association with a further augmentation of GEM-induced accumulation of TAp63 protein but not of TAp73 protein. In contrast to MiaPaCa-2 spheres, *RUNX2* depletion in

MiaPaCa-2 monolayer cultures increased their GEM sensitivity through the potentiation of TAp73-dependent cell death pathway (14). At present, we do not know the precise molecular mechanisms behind RUNX2-mediated differential regulation of TAp73/TAp63 under 2D and 3D sphere culture conditions.

Since *RUNX2* knockdown in MiaPaCa-2 spheres did not affect the *TAp63* transcription level following GEM exposure, TAp63 may be regulated at the protein level. Indeed, TAp63 protein was stabilized in MiaPaCa-2 spheres treated with proteasome inhibitor, and the overexpression of RUNX2 in MiaPaCa-2 spheres reduced TAp63 at the protein level. Notably, Itch which acts as an E3 ubiquitin protein ligase for TAp63 (24), was downregulated in *RUNX2*-depleted MiaPaCa-2 spheres exposed to GEM, indicating that the reduced expression of Itch facilitated the stabilization of TAp63 protein. Levy *et al* (29) indicated that *Itch* promoter contained the consensus RUNX-binding site, and RUNX1 stimulateds the transcription of *Itch*. Based on our results, the knockdown of *RUNX2* had an undetectable effect on *Itch* mRNA level, indicative that, unlike RUNX1, RUNX2 may regulate Itch at the protein level but not at the mRNA level. As proposed (30), Itch was also a potential molecular target of chemotherapy.

Another finding of the present study was that *RUNX2* gene silencing further induced the accumulation of γH2AX in response to GEM. Since ATM-mediated phosphorylation of histone variant H2AX is one of the early molecular events of DNA damage response, RUNX2 may participate in the initial regulatory mechanisms of DNA damage response. Recently, we have also observed a similar phenomenon under 2D cultures demonstrating that depletion of *RUNX2* in MiaPaCa-2 cells increased the accumulation of γH2AX following GEM or SAHA exposure (14,31), indicating that RUNX2 attenuated the expansion of DNA lesions irrespective of 2D or 3D culture systems. Notably, Yang *et al* (32) described that RUNX2 binds to γH2AX and siRNA-mediated knockdown of *RUNX2* increases γH2AX in response to UV. Further studies are required to elucidate the functional significance of RUNX2/γH2AX interaction during DNA damage response.

In conclusion, the results of the present study demonstrated that, similar to 2D cultures, *RUNX2* depletion improved GEM sensitivity of MiaPaCa-2 spheres, and thus strongly indicated that *RUNX2* gene silencing may provide a promising strategy for the treatment of GEM-resistant pancreatic cancer with *p53* mutation.

Acknowledgements

We thank Dr Toshiko Yoshida, Dr Motonori Okabe and Dr Chika Soko for their valuable discussions.

Funding

The present study was supported in part by a grant from the Ministry of Education, Culture, Sports, Science and Technology of Japan (no. 23501278).

Availability of data and materials

The analyzed datasets generated during the study are available from the corresponding author on reasonable request.

Authors' contributions

TO and TN organized the present study. MS, MN, TO and DS performed the experiments. OS contributed to the interpretation of the results. MS and TO were the major-contributors in writing the manuscript. All authors read and approved the manuscript and agree to be accountable for all aspects of the research in ensuring that the accuracy or integrity of any part of the work are appropriately investigated and resolved.

Ethics approval and consent to participate

Not applicable.

Consent for publication

Not applicable.

Competing interests

The authors declare that they have no competing interests.

References

1. Vincent A, Herman J, Schulick R, Hruban RH and Goggins M: Pancreatic cancer. Lancet 378: 607-620, 2011.
2. Neesse A, Algül H, Tuveson DA and Gress TM: Stromal biology and therapy in pancreatic cancer: A changing paradigm. Gut 64: 1476-1484, 2015.
3. Burris HA III, Moore MJ, Andersen J, Green MR, Rothenberg ML, Modiano MR, Cripps MC, Portenoy RK, Storniolo AM, Tarassoff P, *et al*: Improvements in survival and clinical benefit with gemcitabine as first-line therapy for patients with advanced pancreas cancer: A randomized trial. J Clin Oncol 15: 2403-2413, 1997.
4. Ryan DP, Hong TS and Bardeesy N: Pancreatic adenocarcinoma. N Engl J Med 371: 1039-1049, 2014.
5. von Hoff DD, Ervin T, Arena FP, Chiorean EG, Infante J, Moore M, Seay T, Tjulandin SA, Ma WW, Saleh MN, *et al*: Increased survival in pancreatic cancer with nab-paclitaxel plus gemcitabine. N Engl J Med 369: 1691-1703, 2013.
6. Cicenas J, Kvederaviciute K, Meskinyte I, Meskinyte-Kausiliene E, Skeberdyte A and Cicenas J: KRAS, TP53, CDKN2A, SMAD4, BRCA1, and BRCA2 mutations in pancreatic cancer. Cancers 9: E42, 2017.
7. Komori T, Yagi H, Nomura S, Yamaguchi A, Sasaki K, Deguchi K, Shimizu Y, Bronson RT, Gao YH, Inada M, *et al*: Targeted disruption of *Cbfa1* results in a complete lack of bone formation owing to maturational arrest of osteoblasts. Cell 89: 755-764, 1997.
8. Otto F, Thornell AP, Crompton T, Denzel A, Gilmour KC, Rosewell IR, Stamp GW, Beddington RS, Mundlos S, Olsen BR, *et al*: *Cbfa1*, a candidate gene for cleidocranial dysplasia syndrome, is essential for osteoblast differentiation and bone development. Cell 89: 765-771, 1997.
9. Franceschi RT and Xiao G: Regulation of the osteoblast-specific transcription factor, Runx2: Responsiveness to multiple signal transduction pathways. J Cell Biochem 88: 446-454, 2003.
10. Chimge NO and Frenkel B: The RUNX family in breast cancer: Relationships with estrogen signaling. Oncogene 32: 2121-2130, 2013.
11. Cohen-Solal KA, Boregowda RK and Lasfar A: RUNX2 and the PI3K/AKT axis reciprocal activation as a driving force for tumor progression. Mol Cancer 14: 137, 2015.
12. Ozaki T, Wu D, Sugimoto H, Nagase H and Nakagawara A: Runt-related transcription factor 2 (RUNX2) inhibits p53-dependent apoptosis through the collaboration with HDAC6 in response to DNA damage. Cell Death Dis 4: e610, 2013.

13. Sugimoto H, Nakamura M, Yoda H, Hiraoka K, Shinohara K, Sang M, Fujiwara K, Shimozato O, Nagase H and Ozaki T: Silencing of *RUNX2* enhances gemcitabine sensitivity of *p53*-deficient human pancreatic cancer AsPC-1 cells through the stimulation of TAp63-mediated cell death. Cell Death Discov 6: e1914, 2015.
14. Nakamura M, Sugimoto H, Ogata T, Hiraoka K, Yoda H, Sang M, Sang M, Zhu Y, Yu M, Shimozato O and Ozaki T: Improvement of gemcitabine sensitivity of *p53*-mutated pancreatic cancer MiaPaCa-2 cells by *RUNX2* depletion-mediated augmentation of TAp73-dependent cell death. Oncogenesis 5: e233, 2016.
15. Ozaki T, Nakamura M, Ogata T, Sang M, Yoda H, Hiraoka K, Sang M and Shimozato O: Depletion of pro-oncogenic RUNX2 enhances gemcitabine (GEM) sensitivity of p53-mutated pancreatic cancer Panc-1 cells through the induction of pro-apoptotic TAp63. Oncotarget 7: 71937-71950, 2016.
16. Vousden KH and Lu X: Live or let die: The cell's response to p53. Nat Rev Cancer 2: 594-604, 2002.
17. Melino G, De Laurenzi V and Vousden KH: p73: Friend or foe in tumorigenesis. Nat Rev Cancer 2: 605-615, 2002.
18. Hollstein M, Sidransky D, Vogelstein B and Harris CC: p53 mutations in human cancers. Science 253: 49-53, 1991.
19. Reynolds BA and Weiss S: Generation of neurons and astrocytes from isolated cells of the adult mammalian central nervous system. Science 255: 1707-1710, 1992.
20. Hickman JA, Graeser R, de Hoogt R, Vidic S, Brito C, Gutekunst M and van der Kuip H; IMI PREDECT Consortium: Three-dimensional models of cancer for pharmacology and cancer cell biology: Capturing tumor complexity in vitro/ex vivo. Biotechnol J 9: 1115-1128, 2014.
21. Deng L, Li D, Gu W, Liu A and Cheng X: Formation of spherical cancer stem-like cell colonies with resistance to chemotherapy drugs in the human malignant fibrous histiocytoma NMFH-1 cell line. Oncol Lett 10: 3323-3331, 2015.
22. Kuo CT, Wang JY, Lin YF, Wo AM, Chen BPC and Lee H: Three-dimensional spheroid culture targeting versatile tissue bioassays using a PDMS-based hanging drop array. Sci Rep 7: 4363, 2017.
23. Lissy NA, Davis PK, Irwin M, Kaelin WG and Dowdy SF: A common E2F-1 and p73 pathway mediates cell death induced by TCR activation. Nature 407: 642-645, 2000.
24. Rossi M, Aqeilan RI, Neale M, Candi E, Salomoni P, Knight RA, Croce CM and Melino G: The E3 ubiquitin ligase Itch controls the protein stability of p63. Proc Natl Acad Sci USA 103: 12753-12758, 2006.
25. Ren D, Wang M, Guo W, Zhao X, Tu S, Huang S, Zou X and Peng X: Wild-type p53 suppresses the epithelial-mesenchymal transition and stemness in PC-3 prostate cancer cells by modulating miR-145. Int J Oncol 42: 1473-1481, 2013.
26. Cho JH, Kim SA, Park SB, Kim HM and Song SY: Suppression of pancreatic adenocarcinoma upregulated factor (PAUF) increases the sensitivity of pancreatic cancer to gemcitabine and 5FU, and inhibits the formation of pancreatic cancer stem like cells. Oncotarget 8: 76398-76407, 2017.
27. Gao CC, Xu XL, Li F, Gong BG, Liu S, Cui YQ, Sun HC, Xu PY, Zheng YM and Jiang H: Silencing pancreatic adenocarcinoma upregulated factor (PAUF) increases the sensitivity of pancreatic cancer cells to gemcitabine. Tumour Biol 37: 555-564, 2016.
28. Di Fiore R, Marcatti M, Drago-Ferrante R, D'Anneo A, Giuliano M, Carlisi D, De Blasio A, Querques F, Pastore L, Tesoriere G and Vento R: Mutant p53 gain of function can be at the root of dedifferentiation of human osteosarcoma MG63 cells into 3AB-OS cancer stem cells. Bone 60: 198-212, 2014.
29. Levy D, Reuven N and Shaul Y: A regulatory circuit controlling Itch-mediated p73 degradation by Runx. J Biol Chem 283: 27462-27468, 2008.
30. Hansen TM, Rossi M, Roperch JP, Ansell K, Simpson K, Taylor D, Mathon N, Knight RA and Melino G: Itch inhibition regulates chemosensitivity in vitro. Biochem Biophys Res Commun 361: 33-36, 2007.
31. Ogata T, Nakamura M, Sang M, Yoda H, Hiraoka K, Yin D, Sang M, Shimozato O and Ozaki T: Depletion of runt-related transcription factor 2 (RUNX2) enhances SAHA sensitivity of *p53*-mutated pancreatic cancer cells through the regulation of mutant p53 and TAp63. PLoS One 12: e0179884, 2017.
32. Yang S, Quaresma AJ, Nickerson JA, Green KM, Shaffer SA, Imbalzano AN, Martin-Buley LA, Lian JB, Stein JL, van Wijnen AJ and Stein GS: Subnuclear domain proteins in cancer cells support the functions of RUNX2 in the DNA damage response. J Cell Sci 128: 728-740, 2015.